Spatial and temporal dynamics of nano- and pico-size particulate organic matter (POM) in a coastal megatidal marine system

Molly A. Moynihan,[1] Pierrick Barbier,[1] Frédéric Olivier,[1] Nicolas Toupoint,[2] Tarik Meziane*[1]

[1]Unité Mixte de Recherche Biologie des organismes et écosystèmes aquatiques (BOREA UMR 7208), Sorbonne Université, Muséum National d'Histoire Naturelle, Université Pierre et Marie Curie, Institut de Recherche pour le Développement, Université de Caen-Normandie, Université des Antilles, Paris, France
[2]Institut des Sciences de la Mer (ISMER) - Université du Québec à Rimouski (UQAR), Rimouski, Québec, Canada

Abstract

Surface water samples of size-selected seston (0.7–20 μm) were collected from April 2013 to September 2013 at three similar coarse-sand benthic habitats. Additionally, seston sampling was performed at a fixed location throughout a complete tidal cycle (2014). A combination of fatty acid (FA), isotope, and flow cytometry analyses were used to determine the quality and quantity of nano- and pico-sized particulate organic matter (POM). High variability was found between fatty acid replicate samples. Similar temporal patterns were observed at two sheltered sites, while the exposed site displayed less pronounced seasonal changes. Lower concentrations of 16C and 18C polyunsaturated fatty acids were found during low tide sampling. Globally, POM was dominated by picoeukaryotes, with concentrations exceeding 50,000 cells mL^{-1}, and $(16{:}4\omega3 + 18{:}3\omega3)/\Sigma\omega3$ is proposed as novel biomarker of picoeukaryotes in this region.

Organic matter in the ocean occurs in particulate (including colloidal) or dissolved forms. On a global scale, dissolved organic matter (DOM) (<0.5 μm) is 50–100 times more concentrated in seawater than particulate organic matter (POM) (>0.5 μm) (Sharp 1973). However, in coastal environments, POM concentrations are quantitatively more important than DOM due to the high productivity of coastal waters, the increased rate of exchange between sediment and the water column, and terrigenous input (Bodineau et al. 1999). POM is comprised of both living and nonliving matter, including microalgae, bacteria, detritus, fecal pellets, and clays (Volkman and Tanoue 2002). Nonliving POM generally has a biomass 10-times greater than plankton biomass and is dominated by complex carbohydrates that are difficult to decompose (Pomeroy 1980). Living POM components play essential roles in marine food webs and oceanic biogeochemical cycles, through process such as photosynthesis, nitrogen fixation, and remineralization (Falkowski 1994; Voss et al. 2013).

Variability in the quantity and quality of living POM is often due to natural species succession, changes in organism physiology, viral lysis, and nutrient availability (Mayzaud et al. 1989; Leu et al. 2006; Toupoint et al. 2012; Lønborg et al.

2013). Microbial activity on detritus can release nutrients to the water column (Biddanda 1988). Seasonal and daily hydrologic conditions, such as tide, temperature, irradiance, wind and currents, can greatly influence the concentration and composition of living and nonliving suspended POM (Bodineau et al. 1998, 1999; Sakdullah and Tsuchiya 2008; Wyatt et al. 2010). For example, tidal mixing can resuspend sediment, increasing nutrient concentrations for pelagic phytoplankton and adjacent benthic habitats; however, nutrient availability must also coincide with sufficient irradiance for photosynthetic organisms (Sakdullah and Tsuchiya 2008; Schaal et al. 2008).

Recently, the importance of nano- and pico-sized POM components in ocean biogeochemical cycles and ecosystem functioning has come into focus (Not et al. 2004; Bouman et al. 2011; Zehr and Kudela 2011; Buitenhuis et al. 2012; Close et al. 2014). Nanoplankton (2–20 μm) and picoplankton (0.2–2 μm) are significant global primary producers. Not only do they constitute a significant percentage of carbon biomass (Joint et al. 1986; Widdicombe et al. 2010; Buitenhuis et al. 2012; Marañón 2015), but the highest metabolic and growth rates among phytoplankton are found within these two size classes (1–10 μm) (Marañón 2015).

In the English Channel, seasonal phytoplankton dynamics are well documented; smaller phytoplankton are abundant year-round (Not et al. 2004; Widdicombe et al. 2010) and contribute significantly to algal biomass and primary production (Not et al. 2004; Widdicombe et al. 2010;

Additional Supporting Information may be found in the online version of this article.

*Correspondence: meziane@mnhn.fr

Masquelier et al. 2011), while larger sized phytoplankton (e.g., diatoms, dinoflagellates) have intense and ephemeral seasonal blooms (Irigoien et al. 2000; Henson et al. 2006; Van Oostende et al. 2012). While these previous works underline seasonal patterns of nano- and picoplankton in this region, there is a paucity of information on POM dynamics in this size range, particularly in regions with tight benthic-pelagic coupling, such as the western English Channel, where POM is strongly influenced by both living and nonliving phytoplankton and macroalgae (Perez et al. 2013).

Changes in the concentration or quality of this resource can greatly impact marine food webs and primary consumers. In particular, the life cycles of filter feeders are tightly coupled with the nutritional quality and concentration nano- and pico-sized POM (Axiak and George 1987; Sprung and Rose 1988; Raby et al. 1997; Ward et al. 1998; Ward and Shumway 2004; Strohmeier et al. 2012; Kamermans et al. 2013). Within the English Channel, in Mont Saint-Michel Bay (France), estimates show that filter feeders consume 26% of total phytoplankton biomass, exerting a strong top–down control on chlorophyll *a* concentrations (Cugier et al.). Consequently, POM dynamics could indirectly affect the commercial and recreational fisheries that play a key ecological and economic role in this region. The local bivalve harvesting industry produces around 16,000 tons of shellfish, yielding more than 30 million Euros per year (Cugier et al.). In addition, a large number of recreational shellfish harvesters exploit this resource during the spring and summer months (Godet 2008; Godet et al. 2009).

To investigate POM dynamics and its trophic implications at multiple spatial and temporal scales, we combine the fatty acid (FA) marker technique, flow cytometry, and stable isotope analysis. Such a multifaceted approach is particularly helpful in coastal areas, as it can help distinguish the contribution of various primary producers from the overall POM composition (Guest et al. 2010; Kelly and Scheibling 2012). The FA marker technique has been successfully applied to study POM sources in the water column and its transfer along the food web (Mayzaud et al. 1989; Bodineau et al. 1999; Dalsgaard et al. 2003; Kelly and Scheibling 2012). Differences in FA biosynthesis between taxonomic groups have led to the development of FA trophic markers (FATM), which can be used to identify specific groups of organisms and their food sources (Meziane et al. 1997; Dalsgaard et al. 2003). In addition, FA functional groups can be used to broadly characterize POM; for example, the ratio of PUFA/SFA (polyunsaturated FA/saturated FA) is an indicator of trophic resource quality and branched fatty acids (BFA) are indicators of bacteria (Dalsgaard et al. 2003; Meziane et al. 2006). Flow cytometry is complementary to FA analysis, particularly in coastal environments, as it quantifies living pico- and nano- plankton and excludes nonliving macroalgal components (Guzmán et al. 2009; Toupoint et al. 2012). Lastly, stable isotope signatures, δ^{13}C and δ^{15}N, can reflect POM composition, ambient environmental conditions, metabolic processes, or differential diffusion during uptake (Peterson and Fry 1987; McCutchan et al. 2003; Golléty et al. 2010; Wyatt et al. 2010).

This study occurred in the Chausey Archipelago, located within the Mont Saint-Michel Bay. Dynamics of nano- and pico-sized POM were studied at three sites, classified under the same benthic habitat (Godet et al. 2009), from April 2013 to September 2013 and at a fixed location throughout a complete tidal cycle during the spring of 2014. Benthic habitat classification was performed by Godet et al. (2009) based on parameters commonly used in marine conservation (e.g., EUNIS, Natura 2000), whereby biophysical characteristics vary more between than within habitats. Results were used to test our hypotheses that (1) nano- and pico-sized POM composition at Chausey show weak spatial patterns and strong temporal patterns (including within the timescale of a tidal cycle) and (2) flow cytometry and FA data can be combined to highlight potential novel biomarkers of pico- and nano-plankton in this region.

Material and methods

Study site and sampling

Chausey is a highly fragmented, eutrophic environment experiencing a semidiurnal tidal pattern and a maximal tidal range of 14 m. With a spring tidal range greater than 8 m, Chausey is classified as a megatidal environment (Levoy et al. 2000), and over 30% of its sand flats are exposed during extreme low tides (Godet et al. 2009). At all sampling sites, the water column is approximately 10 m during a spring high tide.

In 2013, spatio-temporal variation of POM was studied by sampling surface water suspended matter during each spring tide (tidal range $\geq$ 8 m; every 2–3 weeks) 23rd from April to 21st September, at three intertidal sites in the Chausey Archipelago: (48°52.341N, 1°50.699W), B (48°52.824N, 1°49.931W), C (48°53.281N, 1°47.834W) (Fig. 1). Site A is exposed to westerly swells from the English Channel, whereas both sites B and C are sheltered. Site B is located in the Sound Channel, a marine preserve that prohibits commercial and recreational bivalve harvesting, and site C is adjacent to mussel farms (Grant et al. 2012). All sampling sites were located in the *Glycymeris glycymeris* (dog cockle) coarse sands habitat (Godet 2008). Surface water was sampled 2 h after low tide ($\pm$5 min), when water column depth was approximately 1 m. Four replicates were taken per site (3) and per "sampling week" (10). On 31 March 2014, surface water was sampled seven different instances at fixed a location (TC, Fig. 1) (48°52.895N, 1°49.875W) throughout a complete tidal cycle: high tide (9:20), ebb tide (11:50, 14:20), low tide (16:20), flood tide (18:20, 19:50), and high tide (21:30). The tidal range was over 12 m and three replicates were taken per sampling time.

Surface water samples were collected in dark 8 L bottles and temperature was recorded using an onset HOBO® data logger. Water was prefiltered with a 20 μm mesh. Between 2 L and 4 L of prefiltered water were then filtered on
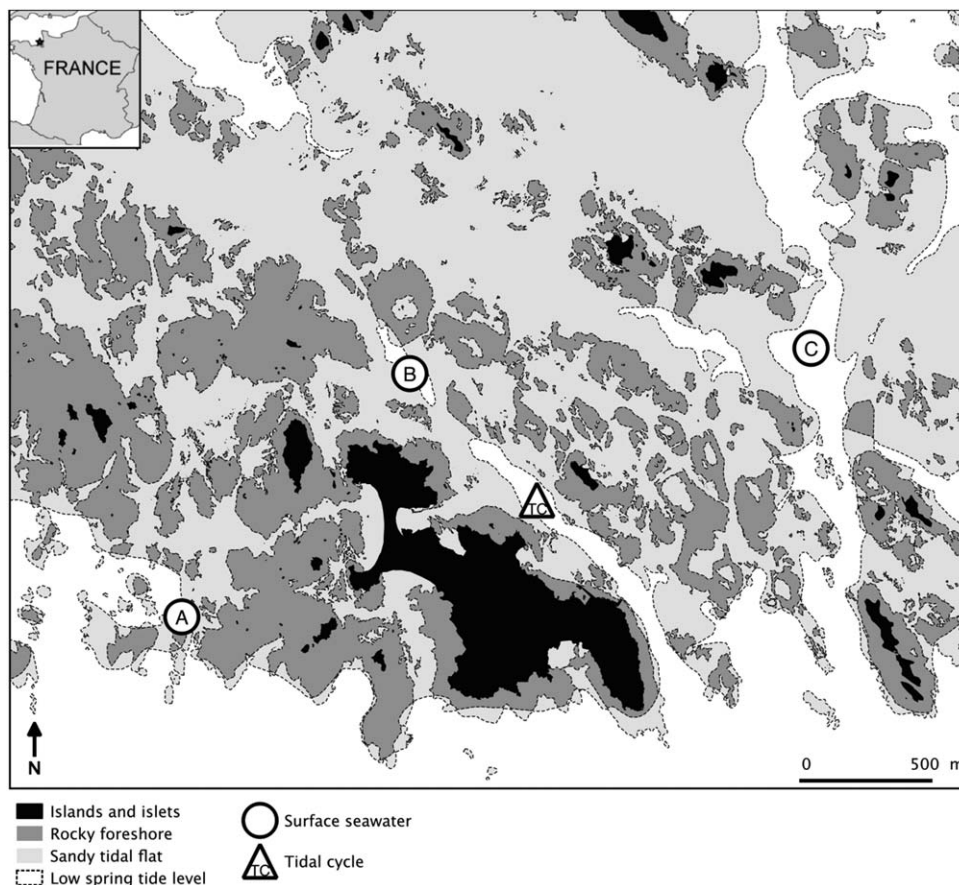
Fig. 1. Map of the Chausey Archipelago, located in the Mont Saint-Michel Bay, Normand-Breton Gulf, France. Circles represent the seasonal 2013 sites (A, B, C), and the triangle is the 2014 tidal cycle site. (Map modified from Godet et al. 2008)

precombusted GF/F 47 mm microfiber filters (Whatman®), capturing particles between 0.7 μm and 20 μm. Filters were immediately stored at $-80°C$ and freeze-dried prior to analysis. For flow cytometry, prefiltered water (4.5 mL) was fixed with glutaraldehyde (Sigma-Aldrich G5882, 0.1% final concentration), frozen, and stored at $-80°C$ until analyzed. In 2013, replicates were performed in quadruplicate for fatty acid, isotope and flow cytometry analyses. During tidal cycle sampling (2014), replicates were performed in triplicate for fatty acid and isotope analyses.

Fatty acid extraction and analysis

Lipids were extracted from filters following a modified method of Bligh and Dyer (1959) as described in Meziane et al. (2006). An internal standard (23:0) was added to the sample prior to extraction. Cholorform was evaporated under nitrogen (N_2) flux. Dried lipid extracts were then saponified with a solution of methanol and sodium hydroxide (NaOH, 2N) (2:1, v:v) at 90°C for 1 h 30 min. Subsequently, methylization was performed, transforming all fatty acid esters into fatty acid methyl esters (FAME) using methanolic boron trifluoride (BF_3—CH_3OH).

FAME were quantified by gas chromatography analysis (Varian 3800), using a flame ionization detector. Identification of fatty acids was performed using coupled gas chromatography mass spectrometry (Varian 450-GC; Varian 220-MS), as well as by comparison of gas chromatography retention times with those of standards (Supelco®).The internal standard (23:0) was used to determine the concentration of each fatty acid (C_{FA}) in μg FA per mg POM. The weight of POM on each filter was determined by subtracting the weight of the precombusted filter from the weight of the freeze-dried filter after sampling. A_{FA} is the area of a given FA peak, A_{23} and Q_{23} are the area and quantity (μg) of the internal standard, and Q_{DW} is the dried weight of POM on the filter (mg). C_{FA} may also be represented in terms of μg FA per L, by replacing Q_{DW} with the volume of seawater filtered (L).

$$C_{FA} = \frac{A_{FA}}{A_{23}} \times \frac{Q_{23}}{Q_{DW}}$$

Stable isotope analysis

POM samples were fumigated for 4 h using 35% HCl to remove all carbonates. Samples were prepared in tin capsules

and analyzed at the University of California Davis Stable Isotope Facility (Department of Plant Sciences, UC Davis, Davis, California), using a Vario EL Cube elemental analyzer (Elementar Analysensysteme GmbH, Hanau, Germany) interfaced to a PDZ Europa 20–20 isotope ratio mass spectrometer (Sercon Ltd., Cheshire, U.K.). During analysis, replicates of compositionally similar laboratory standards previously calibrated against IAEA international Standard Reference Materials were interspersed with samples. Carbon and Nitrogen results are reported in parts per thousand (‰), using standard delta notation (δ^{13}C and δ^{15}N), and are relative to V-PDB (Vienna PeeDee Belemnite) and Air, respectively. R is the ratio of heavier to lighter isotope.

$$\delta^{13}\text{C},\ \delta^{15}\text{N} = \left[\left(\frac{R_{\text{sample}}}{R_{\text{standard}}} \right) - 1 \right] \times 1000$$

Flow cytometry

Using a 488 nm laser (blue), two planktonic communities were determined: eukaryotes, which fluoresce at 690 nm (red), and cyanobacteria, which fluoresce at 570 nm (orange). In each sample, microspheres (1 μm and 2 μm, Fluoresbrite plain YG, Polysciences) were added to distinguish size classes within each group: pico- (0.2–2 μm) and nano- (2–20 μm) plankton (Tremblay et al. 2009). Heterotrophic bacteria samples were stained with SYBR Green I and measured at 525nm to detect low and high nucleic acid content (Belzile et al. 2008). Analyses were performed on an Epics Altra flow cytometer (Beckman Coulter) using Expo32 v1.2b software (Beckman Coulter). Sampled volume was quantified by weighing a sub-sample before and after processing. Average variation coefficients of duplicate samples were 7.4% and 6.4% for phytoplankton and heterotrophic bacteria abundances, respectively.

Statistical analysis

Multivariate analysis was performed using PRIMER V6 (Clarke and Warwick 2001) and R statistical software (R Core Team 2014) to investigate seasonal patterns in FA relative percentages. PERMANOVA was conducted with two-factors (sampling week and sampling site). Similarity percentages (SIMPER) tests were used to compare FA profiles within and between sites. Within each sampling site, a one-way analysis of similarities (ANOSIM) was performed, with sampling week as the factor. The concentrations and ratios of FA functional groups (e.g., MUFA, PUFA) were compared between sites using Student's t-tests and Mann-Whitney-Wilcoxon tests, when parametric conditions were not satisfied. Likewise, isotope data from seasonal sampling were analyzed using a two-way ANOSIM (factors: sampling week and sampling site) and a subsequent one-way ANOSIM for each site (factor: sampling week).

FA relative percentages from tidal cycle sampling were analyzed using ANOSIM and SIMPER. Samples were grouped and tested in two ways, by sampling week (seven groups) and by tidal regime (four groups). Concentrations of FA functional groups (e.g., MUFA, PUFA) were compared using Kruskal-Wallis tests between sampling points and between tidal regimes. Subsequently, principal coordinate analysis was used to determine FAs contributing most to variability within the tidal cycle. Isotope data from tidal sampling in 2014 were compared with seasonal isotope signatures in 2013 using a Mann-Whitney test.

Patterns in flow cytometry results were detected using pair-wise Kendall correlation tests of cell types (nanocyanobacteria, nanoeukaryote, picocyanobacteria, picoeukaryote). The effect of sampling week and sampling site on cell abundances was tested using analysis of variance (ANOVA). Lastly, repeated measures ANOVA tests were performed to investigate differences in cell type between sampling locations, and paired t-tests with a Holm adjustment were used to identify significantly different sites.

Lastly, principal coordinates analysis and distance-based linear models (DistLM) were used to identify possible FA biomarkers of picoeukaryotes, and significance was tested with Pearson's correlations. All statistically significant results are represented by p-values with an alpha less than 0.05.

Results

Environmental conditions

Surface water temperature ranged from 9.7°C to 21.1°C throughout the 2013 sampling season (Fig. 3). The temperature increased approximately 6°C from April to mid-July and then remained stable at 19.3 $\pm$ 0.8°C throughout early September.

Fatty acids

Seasonal

For 2013 sampling, a total of 48 FAME were identified in POM (0.7–20 μm). Table 1 contains data of FA functional groups from site B, which is the site nearest to tidal cycle sampling (2014) (complete FA data in Supporting Information Tables i-iii). Averaged across sites A, B, and C, SFA accounted for 63% to 86% of total FAs. Monounsaturated fatty acids (MUFA) varied from 3% to 16% of total FAs, and PUFA varied from 8% to 18%. Replicate similarity within sites ranged from 72% to 91% with an average of 82.5 $\pm$ 4.6% (SIMPER, Mean $\pm$ SE). BFA varied from 1.4% to 4.5%, with a standard deviation of 0.8% throughout the sampling season.

PERMANOVA results indicate a significant effect of site ($p = 0.001$, pseudo-$F = 5.47$), sampling week ($p = 0.001$, pseudo-$F = 7.67$), and the interaction between site and sampling week ($p = 0.01$, pseudo-$F = 1.65$). A one-way crossed ANOSIM shows significant differences between sites A & B ($p = 0.027$, $R = 0.045$) and A & C ($p = 0.006$, $R = 0.076$). No significant difference was found between sites B & C. The dissimilarities between A & B and A & C were approximately

Table 1. Mean relative percentage (± SE, $n = 4$) of fatty acid (FA) functional groups from particulate organic matter (POM) (0.7–20 μm) sampling at site B. Total FA concentrations are in μg FA per mg POM on filter and μg FA per liter of seawater filtered (± SE, $n = 4$, last two rows). Complete FA datasets are provided in Supporting Information.

Fatty Acids	Apr 23–25	May 22–24	Jun 21–23	Jul 6–8	Jul 20–22	Jul 26–28	Aug 5–7	Aug 18–20	Sep 3–5	Sep 18–21
Relative percentage										
Σ SFA	87.03±0.69	62.02±3.85	79.22±5.39	72.73±3.38	78.66±3.31	78.74±7.46	60.08±2.62	63.71±4.33	78.02±4.84	85.21±4.61
Σ BFA	3.63±0.24	3.44±0.43	3.76±0.28	3.61±0.51	3.83±0.19	3.03±0.54	2.48±0.3	3.31±0.17	3.19±0.49	2.34±0.24
Σ MUFA	2.76±0.81	17.54±2.24	7.67±3.12	11.04±1.61	9.76±1.82	7.97±3.85	16.51±1.44	17.15±1.91	8.08±2.81	5.56±2.47
Σ PUFA	7.49±0.03	17.46±1.99	8.96±1.61	12.31±2.39	7.55±1.91	10.19±2.88	22.00±1.80	16.61±3.15	10.48±1.73	6.57±2.20
Σ ω3	2.94±0.13	12.22±1.39	4.83±1.32	7.81±1.75	4.32±1.08	5.99±2.07	14.73±1.32	9.79±2.21	7.19±1.47	4.41±1.58
Σ ω6	2.63±0.18	2.54±0.31	2.02±0.17	2.10±0.37	1.77±0.43	2.03±0.30	3.31±0.27	3.26±0.39	1.49±0.15	1.06±0.27
Σ Cyclopropanes	0.27±0.05	0.25±0.16	0.30±0.04	0.31±0.07	0.32±0.05	0.42±0.05	0.21±0.06	0.30±0.03	0.28±0.06	0.35±0.03
Total FA concentration										
μg FA/mg POM	1.24±0.32	1.98±0.25	1.21±0.34	3.38±1.02	1.98±0.53	4.45±0.84	8.24±2.96	2.74±0.04	3.63±1.92	2.28±0.25
μg FA/L	2.64±0.58	9.52±0.81	8.44±3.32	9.06±4.27	5.39±0.59	11.02±1.25	17.14±5.16	9.47±3.65	9.11±3.35	11.12±0.95

20% (SIMPER). Higher percentages of SFAs (16:0, 18:0) and lower percentages MUFA (16:1ω7, 18:1ω9, 18:1ω7) and PUFA (18:3ω3, 18:4ω3, 20:5ω3) were found at A in comparison with B and C.

Significant differences in POM FA composition between sequential sampling weeks were found at all three sites (Table 2). Sites B and C display similar patterns, with April & May and May & June having the highest degrees of separation. For all sites, the relative abundance of MUFA (16:1ω7, 18:1ω7, 18:1ω9) and PUFA (18:3ω3, 18:4ω3, 20:5ω3) increased from April to May (SIMPER). Between 26–28 July and 5–7 August, site B displayed significant differences and C was nearly significant. These results can be explained by an increase of MUFA (16:1ω7, 18:1ω7, 18:1ω9) and PUFA (18:3ω3, 18:4ω3, 20:5ω3). An almost identical shift in MUFA and PUFA relative percentages occurred two weeks later at site A (5–7 and 18–20 August); however, 18:3ω3 contributed less to the overall dissimilarity than at B and C.

Seasonally, the highest average total FA concentration was observed at C (8.52 μg FA/mg POM) and the lowest at B (3.11 μg FA/mg POM). Average MUFA and PUFA concentrations at sites A and B did not differ significantly (t-test, $p > 0.05$), whereas concentrations at C were approximately 2.5-fold greater (t-test, $p < 0.05$). SFA concentrations differ significantly at all sites, with C having the highest average concentration and B the lowest. Despite C's high FA concentrations, similar dynamics in FA concentration were observed between sites B and C. The maximal total FA concentration average occurred simultaneously at sites C and B (5th–7th August), whereas at site A, the maximum occurred 2-weeks prior (21st–23rd June). Moreover, ratio of PUFA to SFA does not differ significantly between B and C, with values of 0.20 ± 0.02 and 0.17 ± 0.02 respectively (Mann-Whitney-Wilcoxon, $p > 0.05$, ± SE, $W = 940$). A's PUFA/SFA ratio of 0.13 ± 0.02 is significantly lower than of both B and C (Mann-Whitney-Wilcoxon, $p < 0.05$, ± SE, $W_{AB, AC} = 571$, 509).

Tidal cycle

No significant differences in FA relative percentages were found between the seven sampling points within a tidal cycle (ANOSIM, $n = 3$) (FA data in Supporting Information Table iv). Average dissimilarity between sequential sampling points was low (SIMPER, $n = 3$), with high & ebb, ebb & ebb, ebb & low, and low & flood tides ranging from 16.6% to 18% dissimilarity. Lowest dissimilarities were found between the two flood tide sampling points (6.8%) and flood & high tide (8.5%). Samples collected during flood tide had the lowest amount of variability between replicates. Among replicate samples, ebb and low tide show a higher degree of dissimilarity (19.4% and 18% respectively). ANOSIM based on tidal regime (low tide $n = 3$; ebb, flood, high tides $n = 6$) reveals significant differences between low & flood tide ($p = 0.01$, $R = 0.81$), flood & high tide ($p = 0.01$, $R = 0.36$), and ebb &

Table 2. One-way ANOSIM of fatty acid relative percentages in particulate organic matter (POM) (0.7–20 μm) from sequential sampling weeks in 2013. Results with p-values < 0.6 are in bold. $n = 4$ for each sampling session.

		Apr 23–25	May 22–24	Jun 21–23	Jul 6–8	Jul 20–22	Jul 26–28	Aug 5–7	Aug 18–20	Sep 3–5
		May 22–24	Jun 21–23	Jul 6–8	Jul 20–22	Jul 26–28	Aug 5–7	Aug 18–20	Sep 3–5	Sep 18–21
A	p-value	**0.057**	0.09	0.74	0.94	0.11	0.086	**0.03**	0.51	0.11
	R statistic	**0.54**	0.44	−0.13	−0.17	0.40	0.32	**0.885**	0.01	0.313
B	p-value	**0.03**	**0.03**	0.43	0.57	0.14	**0.03**	0.20	0.34	**0.057**
	R statistic	**0.98**	**0.70**	0.04	−0.04	0.30	**0.47**	0.12	0.05	**0.43**
C	p-value	**0.005**	**0.005**	0.46	0.29	0.43	**0.057**	0.43	0.69	0.09
	R statistic	**1.00**	**0.83**	−0.03	0.04	0.01	**0.58**	−0.02	−0.10	0.32

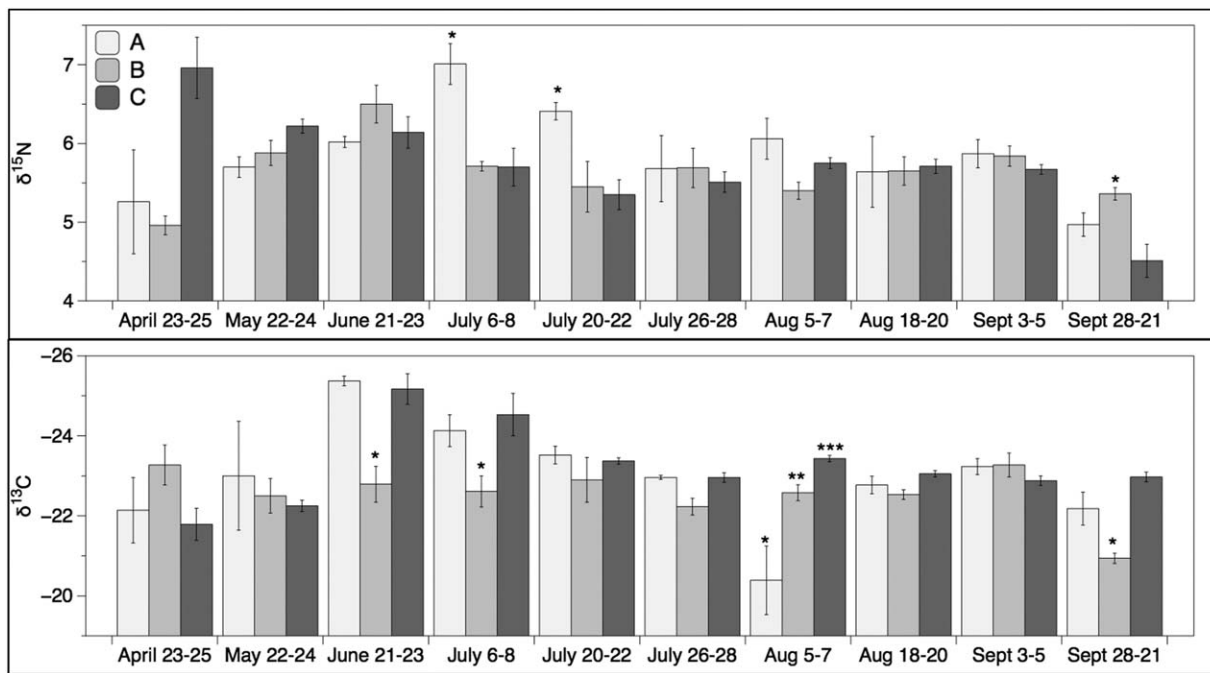**Fig. 2.** Nitrogen (δ^{15}N) and Carbon (δ^{13}C) isotope signatures (mean $\pm$ SE‰) from 2013 nano- and pico-size POM (0.7–20 μm) sampling at sites A, B and C. Asterisks (*) indicate significant differences between sites of the same sampling week.

flood tides ($p = 0.004$, $R = 0.28$). The highest amount of separation was found between low & flood tide ($R = 0.81$).

The total concentration of FAs (μg mg^{-1}) during tidal cycle sampling decreased from ebb tide (0.74 ± 0.07 SE) to low tide (0.52 ± 0.04 SE). However, no significant differences in total FA, SFA, PUFA, MUFA, or BFA concentrations were found between sampling points (Kruskal-Wallis, $p > 0.05$, Chi$^2 > 2.93$). When grouped by tidal regimes, PUFA concentrations varied significantly, with low tide PUFA concentrations differing from all other groups ($p = 0.03$, Chi$^2 = 8.94$, Kruskal-Wallis, post-hoc with Hochberg adjustment). Principal coordinates analysis (PCO, PRIMER) indicated that 16-carbon (16C) and 18-carbon (18C) unsaturated FAs were largely contributing to variability. The sum of 16C PUFA

($p = 0.05$, Chi$^2 = 7.78$) and 18C PUFA ($p = 0.04$, Chi$^2 = 8.30$) concentrations were found to vary significantly with a tidal regime; 16C and 18C PUFA concentrations were significantly lower during low tide, in comparison with high, ebb, and flood tides (Kruskal-Wallis, post-hoc Hochberg adjustment).

Isotopes

In 2013, δ^{13}C and δ^{15}N values of surface water POM across sampling weeks ranged from -25.4 ± 0.1‰ to -20.4 ± 0.9‰ and 4.5 ± 0.2‰ to 7.0 ± 0.3‰ respectively (Fig. 2). Seasonal δ^{13}C (δ^{15}N) signatures averaged -23.1 ± 1.4‰ (5.9 ± 0.7‰), -22.6 ± 0.9‰(5.6 ± 0.5‰), and 23.3 ± 1.0‰ (5.7 ± 0.7‰) for sites A, B, and C respectively. A two-way crossed ANOSIM of sampling week and site illustrates

Table 3. One-way ANOSIM of δ^{15}N and ^{13}C in particulate organic matter (POM) (0.7–20 μm) from sequential sampling weeks in 2013. Results with p-values < 0.6 are in bold. $n = 4$ for each sampling session.

		Apr 23–25	May 22–24	Jun 21–23	Jul 6–8	Jul 20–22	Jul 26–28	Aug 5–7	Aug 18–20	Sep 3–5
		May 22–24	Jun 21–23	Jul 6–8	Jul 20–22	Jul 26–28	Aug 5–7	Aug 18–20	Sep 3–5	Sep 18–21
A	p-value	0.66	**0.03**	**0.03**	0.09	0.09	0.14	0.14	0.54	**0.03**
	R statistic	−0.06	**0.45**	**0.80**	0.20	0.50	0.39	0.30	−0.05	**0.83**
B	p-value	**0.057**	0.43	0.20	0.91	0.74	0.43	0.67	0.11	**0.03**
	R statistic	**0.65**	0.00	0.22	−0.20	−0.11	−0.02	−0.06	0.22	**0.96**
C	p-value	**0.03**	**0.03**	0.46	0.14	0.46	**0.057**	0.09	0.63	**0.03**
	R statistic	**0.59**	**0.98**	−0.04	0.16	0.06	**0.48**	0.35	−0.52	**0.91**

spatial differences, with all pairs of sample sites differing significantly ($p = 0.001$). Sites B and C had the greatest separation ($R = 0.47$), followed by A and C ($R = 0.38$), and B and A ($R = 0.36$). In comparing sequential sampling weeks (normalized, one-way ANOSIM), isotopic compositions of all three sites differed significantly between 3–5 September and 18–21 September ($p < 0.05$, $R > 0.80$) (Table 3).

During tidal cycle sampling (2014), average δ^{13}C and δ^{15}N ranged from -21.3 ± 0.5‰ to -19.8 ± 0.4‰ and 2.9 ± 0.6‰ to 4.1 ± 0.6‰ respectively. No significant difference in isotopic signatures was found throughout the tidal cycle sampling. The isotopic signatures from tidal cycle sampling were significantly ^{13}C enriched and ^{15}N poor relative to POM sampled in 2013 (p-values < 0.001, Mann-Whitney).

Flow cytometry

Picoeukaryotes and Picocyanobacteria account for 57% and 16% of observed variation in cell abundance, respectively ($r^2 = 0.80$, DistLM, PRIMER). Picoeukaryotes dominated flow cytometry results, with an average concentration of $\sim 20{,}000$ cells mL^{-1} throughout the 2013 sampling season (Fig. 3). The highest observed concentration ($>50{,}000$ cells mL^{-1}) occurred at B in early July. All three sites experience a local maxima in May ($\sim 27{,}000$ cells mL^{-1}), followed by a local minima in late June (~ 7000 cells mL^{-1}); this minima coincides with maximal picocyanobacteria concentrations at all sites. Kendall correlation tests of nontransformed data reveal a weak, negative correlation (tau $= -0.215$, $p < 0.001$) between picoeukaryote and picocyanobacteria, whereas all other pair-wise combinations of cell types have weak positive correlations (tau < 0.4, $p < 0.05$).

ANOVA tests on flow cytometry results indicate a significant effect of sampling week ($p < 0.0001$, $F = 286.15$), site ($p < 0.0001$, $F = 16.32$), and of their interaction ($p < 0.0001$, $F = 40.66$). Results from sequential sampling week comparisons are marked in Fig. 3. The effect of sampling site on each cell type was determined using ANOVA repeated measures tests, and inter-site significant differences occurred for nanoeukaryotes ($p = 0.04$, $F = 3.78$), nanocyanobacteria ($p = 0.004$, $F = 5.77$), and picocyanobacteria ($p = 0.003$, $F = 6.18$). Paired t-tests show that sites A & B differed significantly in both pico- and nano-cyanobacteria abundances (Holm adjustment, $p < 0.004$).

Fatty acid biomarkers and picoeukaryotes

Principal coordinates analysis (PCO, PRIMER) was used to simplify the FA dataset into fewer than 15 FAs per sampling site. Using the most abundant cell type, picoeukaryotes, and the simplified FA dataset, a distance-based linear model (DistLM) was applied. Model results suggested a relationship between picoeukaryote concentration and the relative abundance of fatty acids $16{:}4\omega3$, $18{:}3\omega3$, and $20{:}4\omega6$.

Correlation results of potential picoeukaryote FA biomarkers reveal a strong, significant relationship between $(16{:}4\omega3 + 18{:}3\omega3)/\Sigma\omega3$ and picoeukaryote concentrations at sites B and C (Pearson; Table 4). This ratio is correlated with picoeukaryotes at site A, however the relationship is weaker. Relationships were also found between picoeukaryotes and prospective biomarkers $16{:}4\omega3/\Sigma\omega3$ and $18{:}3\omega3/\Sigma\omega3$. A weak, negative correlation was found between $20{:}4\omega6$ and picoeukaryote cell concentrations (Site A $p = 0.008$, $r = -0.43$; Site B $p = 0.07$, $r = -0.30$; Site C $p = 0.01$, $r = -0.42$) (Pearson).

Discussion

Spatial variability

Within all POM samples, high inter-replicate variability and high inter-sampling week similarity were observed in FA compositions. High inter-replicate variability in FA percent compositions has been documented in other spatial-temporal studies (Guest et al. 2010; Wyatt et al. 2010; Kelly and Scheibling 2012). Guest et al. (2010) examined spatial variability in FA profiles between regions, between temperate reefs within a region, and within parts of plants. In all three spatial scales, the greatest variation in FA compositions was found among individual replicates. Our data corroborates such findings, emphasizing the need for multiple replicates and careful sample design.

Here, all three sampling locations were classified under the same benthic habitat (*Glycymeris glycymeris* coarse sands; Godet et al. 2009). With a megatidal regime and the
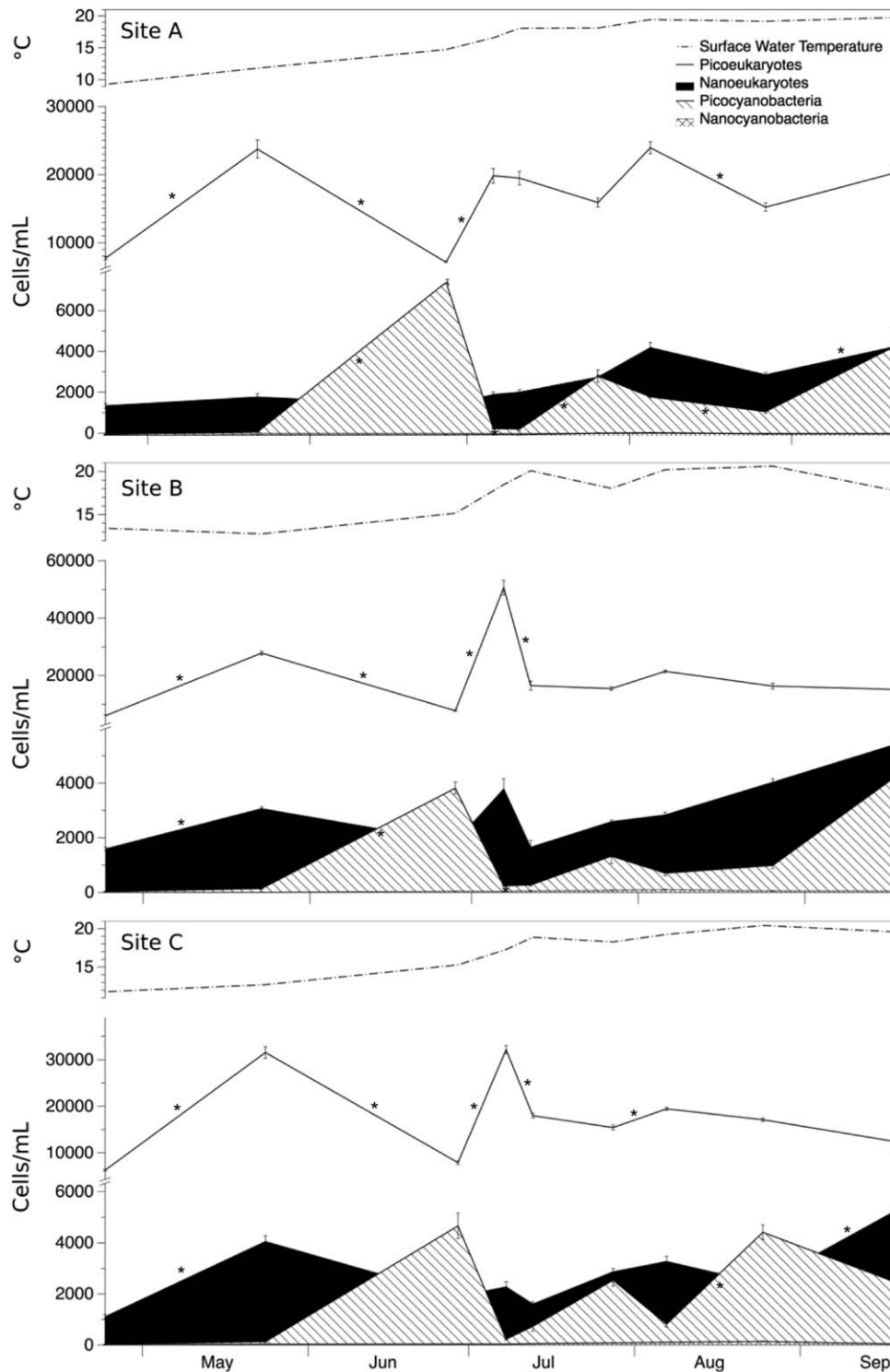
Fig. 3. Flow Cytometry results (mean ± SE cells mL^{-1}) and surface water temperature (°C) for 2013 sampling at sites A, B, and C. Asterisks (*) indicate a significant difference between sequential sampling weeks.

corresponding low water column during spring low tide (<1 m), benthic and pelagic life are very connected. Thus, with similar sediment composition and abundances of benthic species, trophic resource availability was expected to be comparable between sites. Yet, FA and flow cytometry results independently show that POM varies significantly between sites and between sampling weeks. Hydrodynamic differences likely cause the variation between sampling sites.

Table 4. Pearson correlations of potential fatty acid biomarker relative abundances with picoeukaryote cell concentrations for sites A, B, and C. Significant results, *p*-value < 0.5, are in bold (*n* = 36).

	A	B	C
16:4ω3	**r = 0.40**	**r = 0.567**	**r = 0.475**
Σω3	**p = 0.018**	**p = 0.0003**	**p = 0.003**
16:4ω3 ± 18:3ω3	r = 0.302	**r = 0.732**	**r = 0.785**
Σω3	p = 0.08	**p = 3.85e-7**	**p = 1.45e-8**
18:3ω3	r = 0.124	**r = 0.524**	**r = 0.578**
Σω3	p = 0.486	**p = 0.001**	**p = 0.0002**

Small islets shelter both the preserve and mussel farms (B & C), while the remaining site (A) is exposed to westward swells from the English Channel. At the sheltered mussel farm site, high FA concentrations were observed. Mussel farms can alter local hydrodynamics and trap suspended particles between wooden poles (Grant et al. 2012). Moreover, remineralization of mussel biodeposits may also locally influence POM quantity and quality (McKindsey et al. 2011). The preserve, while a no-take fishing zone, is adjacent to the only inhabited island of Chausey, which is frequented by tourists during the summer, and may be subject to small, punctual inputs of bacteria and nutrients from sewage.

Sheltered sites appear to have a similar trophic resource status, as they resemble one another both in their PUFA/SFA ratio and the occurrence of phytoplankton FA biomarker "blooms". Significant differences between sampling weeks are concurrent at these two sites (Table 2). Furthermore, flow cytometry results at sheltered sites are similar, with both sites experiencing a rapid increase and decrease in picoeukaryote abundances during a 14-d period in early July. At the exposed site, picoeukaryote abundances are in accordance with values observed in the literature (Not et al. 2004), but do not attain values > 20,000, as found at sheltered sites. Moreover, the highest average abundance of picocyanobacteria (7500 ± 330cells/mL) was found at the exposed site and is over 1.6-fold the highest abundance at sheltered sites.

Comparatively, while the exposed site is most removed from potential anthropogenic effects, due to its location and the direction of water movement, it exhibited poorer trophic resource quality (low PUFA/SFA), as well as the lowest seasonal variability in trophic resource quality. Lower concentrations of PUFA-rich picoeukaryotes may explain the lesser trophic resource potential of this site. Results may also be related to large wave amplitude, which has been suggested to cause relatively slower bivalve growth (Perez et al. 2013).

Temporal variability

In spite of high inter-replicate variability, POM samples were globally very similar between sampling weeks. For example, all POM samples from April to September in the sheltered preserve had at least 72% similarity. By selecting for smaller POM components (0.7–20 μm), it is possible that marked seasonal signals (e.g., blooms of large diatoms or flagellates > 20 μm) were attenuated, increasing similarity between sampling weeks. Future studies should test this hypothesis, by comparing FA profiles of nano- and pico-POM with profiles from larger size classes and POM as a whole (e.g., > 0.5μm). It is possible that "small-phytoplankton" FA signatures are persistent, yet masked by the dynamics of larger POM constituents. However, here, the selected size range aimed to enhance detection of changes in trophic resources within the nano- and pico-range.

A large diversity of phytoplanktonic species can be found within nano- and pico-sized POM, including small diatoms and dinoflagellates, cyanobacteria, green algae, and haptophytes. At all three sites the relative percentages of diatom (16:1ω7 and 20:5ω3) (Viso and Marty 1993; Meziane et al. 1997; Dalsgaard et al. 2003; Kelly and Scheibling 2012), prasinophyte (18:3ω3) (Dalsgaard et al. 2003), prymnesiophyte (18:4ω3) (Dalsgaard et al. 2003), and dinoflagellate (18:1ω9 and 22:6ω3) (Dalsgaard et al. 2003; Kelly and Scheibling 2012) biomarkers increase from April to May. This observation corroborates previous findings at Chausey in 2011, where Menet-Nedelec et al. (2013) observed a May phytoplankton bloom. This bloom was more pronounced than the March spring bloom (2.5 μ chl*a* L^{-1} vs. 1.5 μ chl*a* L^{-1}, respectively) and dominated by the diatom *Rhizosolenia sp.* (Menet-Nedelec et al. 2013). Our observations at Chausey, along with those of previous authors, differ from classical phytoplankton dynamics in temperate coastal waters, whereby a spring diatom bloom in February/March is followed by rapid nutrient depletion, and subsequent dinoflagellate blooms from spring through summer (May-August) (Gailhard et al. 2002).

The presence of a May phytoplankton bloom at Chausey may be a result of tight benthic-pelagic coupling in the archipelago. Dense bivalve populations can have a top–down effect on POM, reducing concentrations or even changing phytoplankton population dynamics (Prins et al. 1998; Strohmeier et al. 2005, 2008). Moreover, benthic filter feeders consuming pelagic resources transfer material into the sediment, where it can be remineralized and later released into the water column. Bivalve biodeposition and remineralization is well documented in shellfish farming regions, and results in the progressive release of nutrients to the water column, extending primary production into late spring and summer (Prins et al. 1998; Newell et al. 2002; Cugier et al.). Correspondingly, diatom, prasinophyte, prymnesiophyte, and dinoflagellate biomarkers increase in late summer (5–7 August) at the sheltered sites (preserve and mussel bed area) and two weeks later at the exposed site (18–20 August). The presence of such high percentage "blooms" of phytoplankton biomarkers throughout the summer indicates that biodeposition and remineralization

by bivalves may play an important role in phytoplankton dynamics at Chausey (McKindsey et al. 2011).

Among these phytoplankton taxonomic groups, picoeukaryotic prasinophytes (Chlorophyta) are found in high abundances in the English Channel year-round (Not et al. 2004). At Chausey, picoeukaryote abundances were extremely high throughout the sampling season, yet also displayed ephemeral and pronounced fluctuations. In the Western English Channel, Not et al. (2004) observed similar patterns of picoeukaryote concentrations, with abundances of 10,000–20,000 cells mL^{-1} followed by sharp declines to ~2,500 cells mL^{-1}. Large decreases in the picoeukaryote population were found to recover in 15 d (Not et al. 2004). The increase in picoeukaryotes from~ 8,000 cells mL^{-1} to 50,000 cells mL^{-1} in the protected area within a 9-d period suggests that an even more rapid and pronounced changes in picoeukaryote abundances are possible.

Picoplankton communities of mesotrophic environments are characterized by both picoeukaryotes and *Synechococcus* (Zubkov et al. 1998). Enumerated picocyanobacteria at Chausey are thus likely dominated by *Synechococcus* (Marie et al. 2010; Pittera et al. 2014). *Micromonas pusilla*, the most prolific picoeukaryote in the English Channel (Not et al. 2004) is a motile, phototactic prasinophyte (Throndsen 1973; Crawford 1992; Worden and Not 2008). Its ability to respond to a wide range of light conditions may explain its success, particularly in mixed waters (Masquelier et al. 2011). In the coastal Pacific a positive covariance was found between the *Synechococcus* and picoeukaryotes (Worden et al. 2004; Worden and Not 2008). Similarities between *Synechococcus* and picoeukaryote nitrogen uptake may explain this relationship, yet the nature of this relationship is poorly understood (Worden and Not 2008).

While our results do not preclude an underlying positive trend between *Synechococcus* and picoeukaryotes, as observed by Worden et al. (2004), we contrastingly observe a significant negative correlation between picocyanobacteria and picoeukaryotes. For instance, from April to May picoeukaryote and picocyanobacteria concentrations both increase over ~5-fold at the sheltered preserve. However, the sharp decrease in picoeukaryote abundances in June coincides with a ~28-fold increase in picocyanobacteria. Such marked increases in picocyanobacteria, which coincide with local picoeukaryote minima, drive the observed negative correlation between these two cell types. Grazing and viral lysis represent two important causes of mortality for picoeukaryotes (Worden et al. 2004; Worden and Not 2008; Bellec et al. 2009), and in particular, viral lysis may explain observed fluctuations in picoeukaryote abundances in the English Channel (Baudoux et al. 2015).

Worden et al. (2004) observed that 79% of photosynthetic picoplankton grazing occurred on picoeukaryotes, and only 21% on picocyanobacteria (Worden et al. 2004; Worden and Not 2008). The lack of cell wall in some picoeukaryotes,

such as *M. pusilla* and *Ostreococcus* sp., may increase predation pressure on this group of organisms (Worden et al. 2004). Viral lysis of the picoeukaryote *M. pusilla* is known to cause rapid changes in the species' abundance (Mayer and Taylor 1979; Zingone et al. 1999; Lønborg et al. 2013). Furthermore, the abundances of different *M. pusilla* clades are linked to lysis by clade specific prasinoviruses (Baudoux et al. 2015). As viral lysis releases nutrients into the water column, it may stimulate bacteria growth and primary production (Gobler et al. 1997; Brussaard 2004; Lønborg et al. 2013). Given the link between *M. pusilla* abundance and prasinoviral infection, (Mayer and Taylor 1979; Zingone et al. 1999; Not et al. 2004; Lønborg et al. 2013; Baudoux et al. 2015) we hypothesize that viral infection decreases picoeukaryote abundance and allows picocyanobacteria to temporarily thrive in the absence of picoeukaryotic competition. This hypothesis may explain the concurrence of high cyanobacteria concentrations and low picoeukaryote concentrations at Chausey.

While seasonal trends in fatty acids and picoeukaryotes were present, nano- and pico-sized POM within a tidal cycle did not reveal patterns between sampling points. This may be a result of limited replication per week (i.e., $n = 3$). Nonetheless, when samples were grouped into tidal regime, we observe significantly low concentrations of 16C and 18C PUFAs (μg FA/mg POM) during low tide. As both macroalgae and microalgae are rich in 16C and 18C PUFAs, a decrease in one or both of these POM components is likely. This reduction in POM quality may be caused by a decrease in mixing during slack waters, or an increase in resuspended sediment particles collected in low tide samples.

Tidal cycle isotope results differed significantly from all 2013 POM isotope data and evidence seasonality in POM quality. Nitrate (NO_3^-), which is more abundant in the water column in winter and spring, is relatively poor in ^{15}N in comparison with ammonia (NH_4^+) (Wada et al. 1975; Michener and Kaufman 2007). Phytoplankton preferentially consume nitrate and rely on recycled ammonia when nitrate is scarce (Michener and Kaufman 2007). Consequently, seasonal POM studies have found that $\delta^{15}N$ increases from spring to summer, as the system transitions from using ^{15}N poor nitrate to ^{15}N enriched ammonia (Wainright and Fry 1994; Vizzini and Mazzola 2003). $\delta^{15}N$ values during tidal sampling in late-March 2014 were significantly lower in ^{15}N compared with $\delta^{15}N$ values from April through September 2013, suggesting either ammonia usage and nitrogen recycling from late spring to early fall at Chausey or a shift in the dissolved inorganic nitrogen pool between sampling years.

Additionally, $\delta^{13}C$ in late-March (2014) POM was ^{13}C enriched relative to late-April through late-September sampling (2013). Phytoplankton become ^{13}C enriched in bloom conditions (Goering et al. 1990), whereas during summer production, more ^{12}C from respired carbon is available and

δ^{13}C decreases (Rolff 2000). This enrichment suggests that new production was dominant in March (2014) and recycled production from late-April to late-September (2013). Alternatively, differences in carbon isotope signatures could be a result of macroalgae, which are highly abundant at Chausey. As macroalgae δ^{13}C values are more depleted in ^{13}C than POM (Golléty et al. 2010), a greater contribution of macroalgae to nano- and pico-size POM may account for the difference in δ^{13}C between late-March (2014) and late-April to late-September (2013). Lastly, it is unlikely that δ^{13}C was strongly influenced by nearby land, as terrestrial input and salinity variation are very low at Chausey (Menet-Nedelec et al. 2013).

Potential picoeukaryote biomarkers

Both 16:4ω3 and 18:3ω3, which tend to accumulate in prasinophytes (Viso and Marty 1993; Dalsgaard et al. 2003), are positively correlated with picoeukaryote abundances. As the prasinophyte *M. pusilla* is ubiquitous in the English Channel, a correlation between these two FAs and picoeukaryotes is cogent. Of the proposed picoeukaryote FA biomarkers (16:4ω3 + 18:3ω3)/$\Sigma\omega$3 displays the strongest correlation across all sampling sites; however, while the two sheltered sites are commensurate, weaker correlations were found at the exposed site. This result is consistent with observed temporal similarity between sheltered sites. Fluctuations in picoeukaryotes are less substantial at the exposed site, which could make correlations more difficult to ascertain. Further studies of nano- and pico-POM should be performed to validate the potential use of these biomarkers in similar regions, where prasinophytes dominate the picoplankton community. If prasinophytes are not abundant, this biomarker may not be applicable.

Conclusion

Understanding the dynamics of nano- and pico-sized POM is essential to improve the current knowledge of marine food webs and associated fishing industries within this important ecologic and economic region. Between the three sites within the Chausey Archipelago, we observe spatial differences in trophic resource quality and quantity, despite their similar benthic habitat. Sheltered sites appear to have more pronounced seasonal patterns, as well as higher quality trophic resources. At all sites, picoeukaryotes dominated the planktonic component of POM, reaching abundances up to 50,000 cells mL^{-1}.

We propose a novel biomarker, (16:4ω3 + 18:3ω3)/$\Sigma\omega$3, which displayed significant correlations with picoeukaryote abundances. As prasinophytes, specifically *M. pusilla*, are the dominant picoeukaryotes in the English Channel, the proposed ratios may be specific to the class or even genus level. Culture studies should be conducted to test the validity of the new FA biomarkers. Confirming a picoeukaryote biomarker is of great significance to future food web studies, particularly in relation to filter-feeding bivalves, as the rela-

tionship between resource availability, resource quality, and bivalve nutrition is still poorly understood. Results from this study not only provide insight into the seasonality of nano- and pico-sized POM, but also propose new tools, which may be used to further understand resource availability and transfer of picoeukaryotes through marine food webs.

References

Axiak, V., and J. J. George. 1987. Effects of exposure to petroleum hydrocarbons on the gill functions and ciliary activities of a marine bivalve. Mar. Biol. **94**: 241–249. doi:10.1007/BF00392936

Baudoux, A. C., and others. 2015. Interplay between the genetic clades of Micromonasand their viruses in the Western English Channel. Environ. Microbiol. Rep. **7**: 765–773. doi:10.1111/1758-2229.12309

Bellec, L., N. Grimsley, H. Moreau, and Y. Desdevises. 2009. Phylogenetic analysis of new Prasinoviruses (Phycodnaviridae) that infect the green unicellular algae *Ostreococcus*, *Bathycoccus* and *Micromonas*. Environ. Microbiol. Rep. **1**: 114–123. doi:10.1111/j.1758-2229.2009.00015.x

Belzile, C., S. Brugel, C. Nozais, Y. Gratton, and S. Demers. 2008. Variations of the abundance and nucleic acid content of heterotrophic bacteria in Beaufort Shelf waters during winter and spring. J. Mar. Syst. **74**: 946–956. doi:10.1016/j.jmarsys.2007.12.010

Biddanda, B. A. 1988. Microbial aggregation and degradation of phytoplankton-derived detrltus in seawater. 11. Microbial metabolism. Mar. Ecol. Prog. Ser. **42**: 89–95. doi:10.3354/meps042089

Bligh, E. G., and W. J. Dyer. 1959. A rapid method of total lipid extraction and purification. Can. J. Biochem. Physiol. **37**: 911–917. doi:10.1139/y59-099

Bodineau, L., G. Thoumelin, V. Béghin, and M. Wartel. 1998. Tidal time-scale changes in the composition of particulate organic matter within the estuarine turbidity maximum zone in the macrotidal Seine Estuary, France: The use of fatty acid and sterol biomarkers. Estuar. Coast. Shelf Sci. **47**: 37–49. doi:10.1006/ecss.1998.0344

Bodineau, L., G. Thoumelin, and M. Wartel. 1999. Fluxes and seasonal changes in composition of organic matter in the English Channel. Continent. Shelf Res. **19**: 2101–2119. doi:10.1016/S0278-4343(99)00055-2

Bouman, H. A., and others. 2011. Water-column stratification governs the community structure of subtropical marine picophytoplankton. Environ. Microbiol. Rep. **3**: 473–482. doi:10.1111/j.1758-2229.2011.00241.x

Brussaard, C. P. 2004. Viral control of phytoplankton populations—a review. J. Eukaryot. Microbiol. **51**: 125–138. doi:10.1111/j.1550-7408.2004.tb00537.x

Buitenhuis, E. T., and others. 2012. Picophytoplankton biomass distribution in the global ocean. Earth Syst. Sci. Data Discuss. **5**: 221–242. doi:10.5194/essdd-5-221-2012

Clarke, K. R., and R. M. Warwick. 2001. Change in marine communities: An approach to statistical analysis and interpretation, 2nd ed, 172p. PRIMER-E.

Close, H. G., S. G. Wakeham, and A. Pearson. 2014. Lipid and ^{13}C signatures of submicron and suspended particulate organic matter in the Eastern Tropical North Pacific: Implications for the contribution of Bacteria. Deep-Sea Res I. **85**: 15–34. doi:10.1016/j.dsr.2013.11.005

Crawford, D. W. 1992. Metabolic cost of motility in planktonic protist: Theoretical considerations on size scaling and swimming speed. Microb. Ecol. **24**: 1–10. doi:10.1007/BF00171966

Cugier, P., C. Struski, M. Blanchard, J. Mazurié, S. Pouvreau, F. Olivier, J.R. Trigui, E. Thiébaut. 2010. Assessing the role of benthic filter feeders on phytoplankton production in a shellfish farming site: Mont Saint Michel Bay, France. Journal of Marine Systems 82:21:34. doi:10.1016/j.jmarsys.2010.02.013

Dalsgaard, J., M. St John, G. Kattner, D. Müller-Navarra, and W. Hagen. 2003. Fatty acid trophic markers in the pelagic marine environment. Adv. Mar. Biol. **46**: 225–340. doi:10.1016/S0065-2881(03)46005-7

Falkowski, P. G. 1994. The role of phytoplankton photosynthesis in global biogeochemical cycles. Photosynth. Res. **39**: 235–258. doi:10.1007/BF00014586

Gailhard, I., P. Gros, J. P. Durbec, B. Beliaeff, C. Belin, E. Nezan, and P. Lassus. 2002. Variability patterns of microphytoplankton communities along the French coasts. Mar. Ecol. Prog. Ser. **242**: 39–50. doi:10.3354/meps242039

Gobler, C. J., D. A. Hutchins, N. S. Fisher, E. M. Cosper, and S. A. Sanudo-Wilhelmy. 1997. Release and bioavailability of C, N, P Se, and Fe following viral lysis of a marine chrysophyte. Limnol. Oceanogr. **42**: 1492–1504. doi:10.4319/lo.1997.42.7.1492

Godet, L. 2008. L'evaluation des besoins de conservation d'un patrimoine naturel littoral marin: l'exemple des estransmeubles de l'archipel de Chausey. Ph.D. thesis, Muséum nationald'Histoirenaturelle.

Godet, L., J. Fournier, N. Toupoint, and F. Olivier. 2009. Mapping and monitoring intertidal benthic habitats: A review of techniques and a proposal for a new visual methodology for the European coasts. Prog. Phys. Geogr. **33**: 378–402. doi:10.1177/0309133309342650

Goering, J., V. Alexander, and N. Haubenstock. 1990. Seasonal variability of stable carbon and nitrogen isotope ratios of organisms in a North Pacific Bay. Estuar. Coast. Shelf Sci. **30**: 239–260. doi:10.1016/0272-7714(90)90050-2

Golléty, C., P. Riera, and D. Davoult. 2010. Complexity of the food web structure of the *Ascophyllum nodosum* zone evidenced by a δ13C and δ15N study. J. Sea Res. **64**: 304–312. doi:10.1016/j.seares.2010.04.003

Grant, C., P. Archambault, F. Olivier, and C. W. McKindsey. 2012. Influence of "bouchot" mussel culture on the benthic environment in a dynamic intertidal system.

Aquac. Environ. Interact. **2**: 117–131. doi:10.3354/aei00035

Guest, M. A., A. J. Hirst, P. D. Nichols, and S. D. Frusher. 2010. Multi-scale spatial variation in stable isotope and fatty acid profiles amongst temperate reef species: Implications for design and interpretation of trophic studies. Mar. Ecol. Prog. Ser. **410**: 25–41. doi:10.3354/meps08649

Guzmán, H. M., A. Jara Valido, L. C. Duarte, and K. F. Presmanes. 2009. Estimate by means of flow cytometry of variation in composition of fatty acids from *Tetraselmis suecica* in response to culture conditions. Aquac. Int. **18**: 189–199. doi:10.1007/s10499-008-9235-1

Henson, S. A., I. Robinson, J. T. Allen, and J. J. Waniek. 2006. Effect of meteorological conditions on interannual variability in timing and magnitude of the spring bloom in the Irminger Basin, North Atlantic. Deep-Sea Res. I: Oceanogr. Res. Pap. **53**: 1601–1615. doi:10.1016/j.dsr.2006.07.009

Irigoien, X., R. P. Harris, R. N. Head, and D. Harbour. 2000. North Atlantic Oscillation and spring bloom phytoplankton composition in the English Channel. J. Plankton Res. **22**: 2367–2371. doi:10.1093/plankt/22.12.2367

Joint, I. R., N. Owens, and A. J. Pomroy. 1986. Seasonal production of photosynthetic picoplankton and nanoplankton in the Celtic Sea. Mar. Ecol. Prog. Ser. **28**: 1–258. doi:10.3354/meps028251

Kamermans, P., E. Brummelhuis, and M. Dedert. 2013. Effect of algae- and silt concentration on clearance- and growth rate of the razor clam *Ensis directus*, Conrad. J. Exp. Mar. Bio. Ecol. **446**: 102–109. doi:10.1016/j.jembe.2013.05.005

Kelly, J. R., and R. E. Scheibling. 2012. Fatty acids as dietary tracers in benthic food webs. Mar. Ecol. Prog. Ser. **446**: 1–22. doi:10.3354/meps09559

Leu, E., S. Falk-Petersen, S. Kwaśniewski, A. Wulff, K. Edvardsen, and D. O. Hessen. 2006. Fatty acid dynamics during the spring bloom in a High Arctic fjord: Importance of abiotic factors versus community changes. Can. J. Fish. Aquat. Sci. **63**: 2760–2779. doi:10.1139/f06-159

Levoy, F., E. J. Anthony, O. Monfort, and C. Larsonneur. 2000. The morphodynamics of megatidal beaches in Normandy, France. Mar. Geol. **171**: 39–59. doi:10.1016/S0025-3227(00)00110-9

Lønborg, C., M. Middelboe, and C. P. D. Brussaard. 2013. Viral lysis of *Micromonas pusilla*: Impacts on dissolved organic matter production and composition. Biogeochemistry **116**: 231–240. doi:10.1007/s10533-013-9853-1

Marañón, E. 2015. Cell size as a key determinant of phytoplankton metabolism and community structure. Annu. Rev. Mar. Sci. **7**: 241–264. doi:10.1146/annurev-marine-010814-015955

Marie, D., X. L. Shi, F. Rigaut-Jalabert, and D. Vaulot. 2010. Use of flow cytometric sorting to better assess the diversity of small photosynthetic eukaryotes in the English Channel. FEMS Microbiol. Ecol. **72**: 165–178. doi:10.1111/j.1574-6941.2010.00842.x

Masquelier, S., E. Foulon, F. Jouenne, M. Ferréol, C. P. D. Brussaard, and D. Vaulot. 2011. Distribution of eukaryotic plankton in the English Channel and the North Sea in summer J. Sea Res. **66**: 111–122. doi:10.1016/j.seares.2011.05.004

Mayer, J. A., and F. Taylor. 1979. A virus which lyses the marine nanoflagellate *Micromonas pusilla*. Nature **281**: 299–301. doi:10.1038/281299a0

Mayzaud, P., J. P. Chanut, and R. G. Ackman. 1989. Seasonal changes of the biochemical composition of marine particulate matter with special reference to fatty acids and sterols. Mar. Ecol. Prog. Ser. **56**: 189–204. doi:10.3354/meps056189

McCutchan, J. H., W. M. Lewis, C. Kendall, and C. C. McGrath. 2003. Variation in trophic shift for stable isotope ratios of carbon, nitrogen, and sulfur. Oikos **102**: 378–390. doi:10.1034/j.1600-0706.2003.12098.x

McKindsey, C. W., P. Archambault, M. D. Callier, and F. Olivier. 2011. Influence of suspended and off-bottom mussel culture on the sea bottom and benthic habitats: A review. Can. J. Zool. **89**: 622–646. doi:10.1139/z11-037

Menet-Nedelec, F., and others. 2013. Réseau Hydrologique Littoral Normand (RHLN)—Année 2011. Available from http://dx.doi.org/10.13155/28420

Meziane, T., L. Bodineau, C. Retiere, and G. Thoumelin. 1997. The use of lipid markers to define sources of organic matter in sediment and food web of the intertidal salt-marsh-flat ecosystem of Mont-Saint-Michel Bay, France. J. Sea Res. **38**: 47–58. doi:10.1016/S1385-1101(97)00035-X

Meziane, T., F. d'Agata, and S. Y. Lee. 2006. Fate of mangrove organic matter along a subtropical estuary: Small-scale exportation and contribution to the food of crab communities. Mar. Ecol. Prog. Ser. **312**: 15–27. doi:10.3354/meps312015

Michener, R. H., and L. Kaufman. 2007. Stable isotope ratios as tracers in marine food webs. *In* R. Michener and K. Lajtha [eds.], Stable isotopes in ecology and environmental science, 2nd ed., Blackwell Publishing Ltd. doi:10.1002/9780470691854.ch9

Newell, R. I., J. C. Cornwell, and M. S. Owens. 2002. Influence of simulated bivalve biodeposition and microphytobenthos on sediment nitrogen dynamics: A laboratory study. Limnol. Oceanogr. **47**: 1367–1379. doi:10.4319/lo.2002.47.5.1367

Not, F., M. Latasa, D. Marie, T. Cariou, D. Vaulot, and N. Simon. 2004. A single species, *Micromonas pusilla* (Prasinophyceae), dominates the eukaryotic picoplankton in the Western English Channel. Appl. Environ. Microbiol. **70**: 4064–4072. doi:10.1128/AEM.70.7.4064-4072.2004

Perez, V., F. Olivier, R. Tremblay, U. Neumeier, J. Thébault, L. Chauvaud, and T. Meziane. 2013. Trophic resources of the bivalve, *Venus verrucosa*, in the Chausey archipelago (Normandy, France) determined by stable isotopes and fatty acids. Aquat. Living Resour. **26**: 229–239. doi:10.1051/alr/2013058

Peterson, B. J., and B. Fry. 1987. Stable isotopes in ecosystem studies. Annu. Rev. Ecol. Systemat. **18**: 293–320. doi:10.1146/annurev.es.18.110187.001453

Pittera, J., F. Humily, M. Thorel, D. E. Grulois, L. Garczarek, and C. Six. 2014. Connecting thermal physiology and latitudinal nichepartitioning in marine *Synechococcus*. ISME J. **8**: 1221–1236. doi:10.1038/ismej.2013.228

Pomeroy, L. R. 1980. Detritus and its role as a food source, p. 84–102. In R. S. K. Barnes and K. H. Mann [eds.], Fundamentals of aquatic ecosystems. Blackwell Scientific Publishers.

Prins, T. C., A. C. Smaal, and R. F. Dame. 1998. A review of the feedbacks between bivalve grazing and ecosystem processes. Aquat. Ecol. **31**: 349–359. doi:10.1023/A:1009924624259

R Core Team. 2014. R: A language and environment for statistical computing. R Foundation for Statistical Computing. Available from fhttp://www.Rproject.org/

Raby, D., M. Mingelbier, J. J. Dodson, B. Klein, and Y. Lagadeuc. 1997. Food-particle size and selection by bivalve larvae in a temperate embayment—Springer. Mar. Biol. **127**: 665–672. doi:10.1007/s002270050057

Rolff, C. 2000. Seasonal variation in δ13C and δ15N of size-fractionated plankton at a coastal station in the northern Baltic proper. Mar. Ecol. Prog. Ser. **203**: 47–65. doi:10.3354/meps203047

Sakdullah, A., and M. Tsuchiya. 2008. The origin of particulate organic matter and the diet of tilapia from an estuarine ecosystem subjected to domestic wastewater discharge: Fatty acid analysis approach. Aquat. Ecol. **43**: 577–589. doi:10.1007/s10452-008-9195-6

Schaal, G., P. Riera, and C. Leroux. 2008. Trophic coupling between two adjacent benthic food webs within a man-made intertidal area: A stable isotopes evidence. Estuar. Coast. Shelf Sci. **77**: 523–534. doi:10.1016/j.ecss.2007.10.008

Sharp, J. H. 1973. Size classes of organic carbon in seawater. Limnol. Oceanogr. **18**: l–447. doi:10.4319/lo.1973.18.3.0441

Sprung, M., and U. Rose. 1988. Influence of food size and food quantity on the feeding of the mussel *Dreissena polymorpha*. Oecologia **77**: 526–532. doi:10.1007/BF00377269

Strohmeier, T., J. Aure, A. Duinker, T. Castberg, A. Svardal, and O. Strand. 2005. Flow reduction, seston depletion, meat content and distribution of diarrhetic shellfish toxins in a long-line blue mussel (*Mytilus edulis*) farm. J. Shellfish Res. **24**: 15–23. doi:10.2983/0730-8000(2005)24[15:FRSDMC]2.0.CO;2

Strohmeier, T., A. Duinker, O. Strand, and J. Aure. 2008. Temporal and spatial variation in food availability and meat ratio in a longline mussel farm (*Mytilus edulis*). Aquaculture **276**: 83–90. doi:10.1016/j.aquaculture.2008.01.043

Strohmeier, T., Ø. Strand, M. Alunno-Bruscia, A. Duinker, and P. J. Cranford. 2012. Variability in particle retention

efficiency by the mussel *Mytilus edulis*. J. Exp. Mar. Bio. Ecol. **412**: 96–102. doi:10.1016/j.jembe.2011.11.006

Throndsen, J. 1973. Motility in some marine nanoplankton flagellates. Norwegian J. Zool. **21**: 193–200.

Toupoint, N., L. Gilmore-Solomon, F. Bourque, B. Myrand, F. Pernet, F. Olivier, and R. Tremblay. 2012. Match/mismatch between the *Mytilus edulis* larval supply and seston quality: Effect on recruitment. Ecology **93**: 1922–1934. doi:10.1890/11-1292.1

Tremblay, G., C. Belzile, M. Gosselin, M. Poulin, S. Roy, and J. E. Tremblay. 2009. Late summer phytoplankton distribution along a 3500 km transect in Canadian Arctic waters: Strong numerical dominance by picoeukaryotes. Aquat. Microb. Ecol. **54**: 55–70. doi:10.3354/ame01257

Van Oostende, N., J. Harlay, B. Vanelslander, L. Chou, W. Vyverman, and K. Sabbe. 2012. Phytoplankton community dynamics during late spring coccolithophore blooms at the continental margin of the Celtic Sea (North East Atlantic, 2006–2008). Progr. Oceanogr. **104**: 1–16. doi:10.1016/j.pocean.2012.04.016

Viso, A. C., and J. C. Marty. 1993. Fatty acids from 28 marine microalgae. Phytochemistry **34**: 1521–1533. doi:10.1016/S0031-9422(00)90839-2

Vizzini, S., and A. Mazzola. 2003. Seasonal variations in the stable carbon and nitrogen isotope ratios (13C/12C and 15N/14N) of primary producers and consumers in a western Mediterranean coastal lagoon. Mar. Biol. **142**: 1009–1018. doi:10.1007/s00227-003-1027-6

Volkman, J. K., and E. Tanoue. 2002. Chemical and biological studies of particulate organic matter in the ocean. J. Oceanogr. **58**: 265–279. doi:10.1023/A:1015809708632

Voss, M., H. W. Bange, J. W. Dippner, J. J. Middelburg, J. P. Montoya, and B. Ward. 2013. The marine nitrogen cycle: Recent discoveries, uncertainties and the potential relevance of climate change. Philos. Trans. R. Soc. B: Biol. Sci. **368**: 20130121–20130121. doi:10.1098/rstb.2013.0121

Wada, E., T. Kadonaga, and S. Matsuo. 1975. 15N abundance in nitrogen of naturally occurring substances and global assessment of denitrification from isotopic viewpoint. Geochem. J. **9**: 139–148. doi:10.2343/geochemj.9.139

Wainright, S. C., and B. Fry. 1994. Seasonal variation of the stable isotopic compositions of coastal marine plankton from Woods Hole, Massachusetts and Georges Bank. Estuaries **17**: 552–560. doi:10.2307/1352403

Ward, J. E., J. S. Levinton, S. E. Shumway, and T. Cucci. 1998. Particle sorting in bivalves: In vivo determination of the pallial organs of selection. Mar. Biol. **131**: 283–292. doi:10.1007/s002270050321

Ward, E. J., and S. E. Shumway. 2004. Separating the grain from the chaff: Particle selection in suspension- and deposit-feeding bivalves. J. Exp. Mar. Biol. Ecol. **300**: 83–130. doi:10.1016/j.jembe.2004.03.002

Widdicombe, C. E., D. Eloire, D. Harbour, R. P. Harris, and P. J. Somerfield. 2010. Long-term phytoplankton community dynamics in the Western English Channel. J. Plankton Res. **32**: 643–655. doi:10.1093/plankt/fbp127

Worden, A. Z., J. K. Nolan, and B. Palenik. 2004. Assessing the dynamics and ecology of marine picophytoplankton: The importance of the eukaryotic component. Limnol. Oceanogr. **49**: 168–179. doi:10.4319/lo.2004.49.1.0168

Worden, A. Z., and F. Not. 2008. Ecology and Diversity of Picoeukaryotes, p. 159-205. In D.L Kirchman [ed.], Microbial Ecology of the Oceans. John Wiley & Sons, Inc. doi:10.1002/9780470281840.ch6

Wyatt, A., R. J. Lowe, S. Humphries, and A. M. Waite. 2010. Particulate nutrient fluxes over a fringing coral reef: Relevant scales of phytoplankton production and mechanisms of supply. Mar. Ecol. Prog. Ser. **405**: 113–130. doi:10.3354/meps08508

Zehr, J. P., and R. M. Kudela. 2011. Nitrogen cycle of the open ocean: From genes to ecosystems. Annu. Rev. Mar. Sci. **3**: 197–225. doi:10.1146/annurev-marine-120709-142819

Zingone, A., D. Sarno, and G. Forlani. 1999. Seasonal dynamics in the abundance of *Micromonas pusilla* (Prasinophyceae) and its viruses in the Gulf of Naples (Mediterranean Sea). J. Plankton Res. **21**: 2143–2159. doi:10.1093/plankt/21.11.2143

Zubkov, M. V., M. A. Sleigh, G. A. Tarran, P. H. Burkill, and R. J. Leakey. 1998. Picoplanktonic community structure on an Atlantic transect from 50 N to 50 S. Deep-Sea Res. I **45**: 1339–1355. doi:10.1016/S0967-0637(98)00015-6